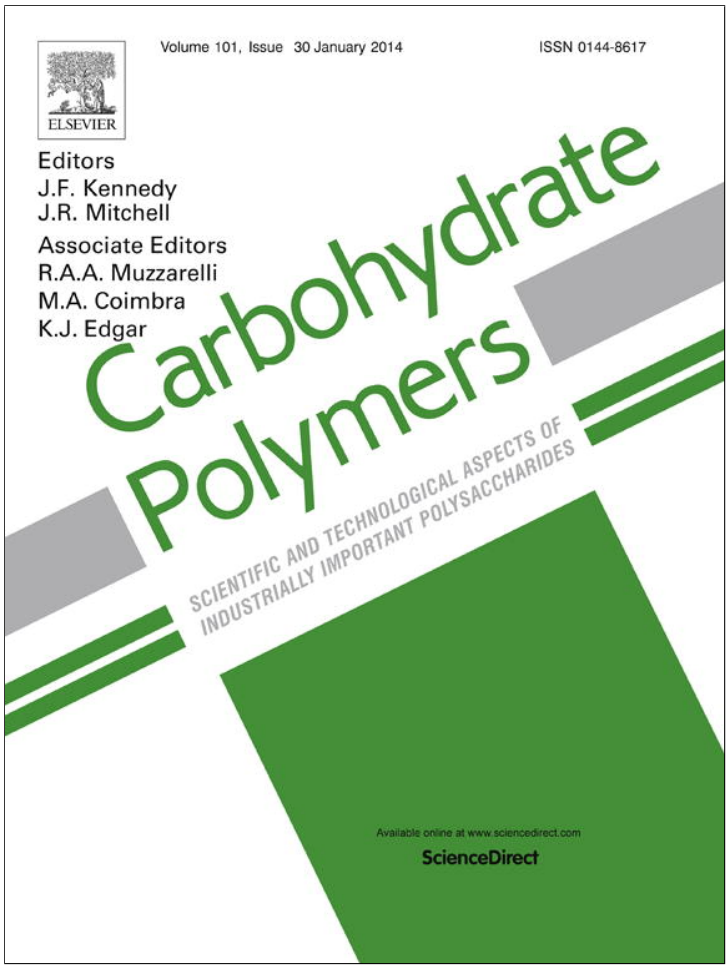

Carbohydrate Polymers 101 (2014) 1018–1026

Contents lists available at ScienceDirect

Carbohydrate Polymers

journal homepage: www.elsevier.com/locate/carbpol

Polyelectrolyte films based on chitosan/olive oil and reinforced with cellulose nanocrystals

Mariana Pereda[a,b], Alain Dufresne[b], Mirta I. Aranguren[a], Norma E. Marcovich[a,*]

[a] Institute of Material Science and Technology (INTEMA), National University of Mar del Plata, Juan B. Justo 4302, 7600 Mar del Plata, Argentina
[b] The International School of Paper, Print Media and Biomaterials (Pagora), Grenoble Institute of Technology, CS10065, F-38402 Saint Martin d'Hères Cedex, France

ARTICLE INFO

Article history:
Received 26 July 2013
Received in revised form 9 October 2013
Accepted 11 October 2013
Available online 22 October 2013

Keywords:
Emulsion films
Chitosan
Olive oil
Cellulose nanocrystals

ABSTRACT

Composite films designed as potentially edible food packaging were prepared by casting film-forming emulsions based on chitosan/glycerol/olive oil containing dispersed cellulose nanocrystals (CNs). The combined use of cellulose nanoparticles and olive oil proved to be an efficient method to reduce the inherently high water vapor permeability of plasticized chitosan films, improving at the same time their tensile behavior. At the same time, it was found that the water solubility slightly decreased as the cellulose content increased, and further decreased with oil addition. Unexpectedly, opacity decreased as cellulose content increased, which balanced the reduced transparency due to lipid addition. Contact angle decreased with CN addition, but increased when olive oil was incorporated. Results from dynamic mechanical tests revealed that all films present two main relaxations that could be ascribed to the glycerol- and chitosan-rich phases, respectively. The response of plasticized chitosan–nanocellulose films (without lipid addition) was also investigated, in order to facilitate the understanding of the effect of both additives.

1. Introduction

Petrochemical-based polymers predominate in food packaging due to their easy processing, excellent barrier properties, and low cost. However, environmental concerns enhance and stimulate the use of renewable resources for producing economically convenient applications that could also improve life quality (García, Pinottia, Martino, & Zaritzky, 2004). In particular, chitosan, the N-deacetylated form of chitin, is a natural cationic polysaccharide, which is edible, non-toxic, biodegradable and commercially available, that has been employed in a variety of applications (Muzzarelli, 2010). Most of the naturally occurring polysaccharides, e.g. cellulose, dextran, pectin, alginic acid, agar, agarose and carrageenans, are neutral or acidic in nature, whereas chitin and chitosan are examples of cationic polysaccharides (Muzzarelli et al., 2012). Moreover, chitosan is also well-known for its broad antimicrobial activity against bacteria and fungi (Cagri, Ustunol, & Ryser, 2004; Muzzarelli et al., 1990) and its ability to act as stabilizer for hydrocolloids–lipids mixtures, promoting emulsion formation and interfacial stabilization. Chitosan films have a low permeability to gases (CO_2 and O_2) and good mechanical properties. However, due to their hydrophilic nature, they are poor barriers to moisture, which limits their use in applications where the control of moisture transfer is desirable, for example prospective food coating/packaging (Ojagh, Rezaei, Razavi, & Hosseini, 2010). The need to use plasticizing agents to obtain stretchable films (Kowalczyk & Baraniak, 2011; Valenzuela, Abugoch, & Tapia, 2013) aggravates this drawback.

To improve the water-barrier properties of hydrocolloid-based films, lipid compounds are frequently incorporated into these structures (Valenzuela et al., 2013; Vargas, Albors, Chiralt, & González-Martínez, 2009), causing a decrease in the water vapor permeability (WVP) values, sometimes at the expense of sensorial alterations that have been shown to characterize foods coated with composite films featuring high amounts of lipids such as saturated acids and waxes (Perez-Gago, Rojas, & Del Rio, 2002; Tanada-Palmu & Grosso, 2005). On the other hand, some authors have reported composite films featuring unsaturated oils rich in oleic acid that can potentially improve the moisture-barrier properties of hydrophilic films and prevent at the same time, drastic changes in their mechanical properties. Moreover, the liquid nature of oils at room temperature makes them easily mixable with biopolymers (Ghanbarzadeh & Almasi, 2011; Pereda, Ponce, Marcovich, Ruseckaite, & Martucci, 2011). When hydrocolloid and lipid ingredients are combined, they may interact favorably, resulting in edible films with improved structural and functional properties,

* Corresponding author. Tel.: +54 223 481 6600; fax: +54 223 481 0046.
E-mail address: marcovic@fi.mdp.edu.ar (N.E. Marcovich).

0144-8617/$ – see front matter © 2013 Elsevier Ltd. All rights reserved.
http://dx.doi.org/10.1016/j.carbpol.2013.10.046

as the mechanical and barrier properties depend not only on the compounds used for the polymer matrix but also on their compatibility (Valenzuela et al., 2013). In this work, olive oil was selected as the lipid to be used to improve barrier properties because of its nutritional value and organoleptics characteristics. It is a vegetable oil, whose monounsaturated fatty acid content (MUFA) is very high (between 56.3 and 86.5%), particularly oleic acid, and it is also rich in tocopherols and phenolic substances, which act as antioxidants.

On the other hand, cellulose nanocrystals (CNs) have attracted significant attention because they are renewable and environmentally benign, naturally abundant, biodegradable, biocompatible and have excellent mechanical properties. CN was shown to reinforce polymers due to the formation of a percolating network that connects the well-dispersed nanofibers by hydrogen bonds (Favier, Chanzy, & Cavaille, 1995). It was shown that the presence of CN in the polymer matrix provides superior performances such as mechanical and barrier properties, leading to the next generation of biodegradable materials (Cao, Chen, Chang, Muir, & Falk, 2008; Dieter-Klemm et al., 2009; Fernandes et al., 2010; Khan et al., 2012). In fact, research in the area of barrier membranes based on cellulosic nanoparticles is now burgeoning.

Therefore, the objective of this work was to evaluate the combined use of cellulose nanoparticles and olive oil to reduce the water vapor permeability of chitosan films intended as edible food packaging, improving at the same time, their mechanical properties. The response of chitosan–nanocellulose films (without lipid addition) was also discussed, in order to facilitate the understanding of the effect of both additives.

2. Experimental

2.1. Materials

Chitosan (CH) (degree of deacetylation 98%, Mv = 1.61 × 10^5 g/mol), supplied by PARAFARM, Mar del Plata, Argentina was used as received. Glycerol (Gly) purchased from Sigma–Aldrich was used as plasticizer. Olive oil (OO) (100% purity, extra virgin, i.e. containing no more than 0.8% acidity, Carrefour brand) was bought in a food market (Grenoble, France). Cotton nanocrystals (CNs) were prepared from commercial cotton paper, previously ground down to fine fibers using a mechanical grinding machine. The chemical procedure for this treatment was as follows:

- *Alkaline treatment* was performed to purify cellulose by removing other constituents present in the cotton fibers. This treatment was carried out by mechanically agitating the cotton fibers into a NaOH solution (2 wt.%) at room temperature and at constant speed for a period of 13 h. After the base treatment, the fibers were filtered through a 40 μm nylon cloth and washed with distilled water until a neutral pH was achieved and all of the alkali solution was completely removed.
- *Fiber hydrolysis* was carried out by mixing the cotton fibers with a concentrated H_2SO_4 solution (65 wt.%) at 45 °C for 45 min, with continuous magnetic stirring. The suspension obtained after hydrolysis was washed with distilled water until neutrality by successive centrifugations (around five times) of 20 min at 10,000 rpm and at 4 °C, and then dialyzed against distilled water. Finally the dialyzed suspension was dispersed using a sonifier (Branson Sonifier 250). The CN dispersion was treated with a drop of chloroform to prevent bacterial growth and then stored in the fridge. The final suspension had a concentration of 1.79 wt.%.

2.2. Methods

2.2.1. Preparation of composite films

The films were prepared by casting, all containing glycerol in a weight ratio Gly/CH = 0.28. CH solutions (2%, wt./v) were prepared in acetic acid (1%, v/v). An appropriate volume of the CN suspension (to obtain final films with 1–12 wt.% nanocellulose) was then dispersed into the CH solution, using a homogenizer (Ultra-Turrax, 3 min treatment) and a sonifier (BRANSON 250, four cycles of 5 min each). For the films containing olive oil, the lipid fraction was incorporated to the former suspension with an OO/CH weight ratio of 0.1, and stable emulsions were achieved by using again both the homogenizer and the sonifier. The film-forming dispersions/emulsions were defoamed under rest for one hour at room temperature and then they were poured into Teflon Petri dishes (diameter = 9 cm) and dried at 35 °C for approximately 15 h in a convection oven. After water was evaporated, the obtained films were peeled off from the plates and kept in a closed room at constant relative humidity (50% RH) and temperature (23 ± 2 °C) for 3 days before testing.

2.2.2. Optical properties

The film forming emulsions were analyzed by transmission optic microscopy (TOM), using a microscope (Leica DMLB) coupled to a video camera (Leica DC100). For this purpose, a drop of the emulsions was placed between glass-holder and glass-cover and pictures were taken at different magnifications.

The color of the films was determined with a NoviBond Colorimeter RT500 (Neu-Isenberg, Germany) with an 8 mm diameter measuring area. A white standard color plate for the instrument calibration was used as a background for color measurement of the films. Results were expressed as L^*, a^* and b^* (lightness '*L*', red–green '*a*' and yellow–blue '*b*') coordinates of the color space CIELab (Gennadios, Weller, Hanna, & Froning, 1996; Kunte, Gennadios, Cuppett, Hanna, & Weller, 1997), that were used to measure lightness, redness, and yellowness. The measured coordinates were used to calculate total color difference (ΔE) with respect to the control CH film and whiteness index (WI), as given by Eqs. (1) and (2) (Monedero, Fabra, Talens, & Chiralt, 2009):

$$\Delta E = \sqrt{(\Delta a^*)^2 + (\Delta b^*)^2 + (\Delta L^*)^2} \quad (1)$$

$$\mathrm{WI} = 100 - \sqrt{(100 - L^*)^2 + a^{*2} + b^{*2}} \quad (2)$$

The opacity is the degree to which light is not allowed to pass through a material. The higher the opacity, the lower the amount of light that can pass through the material (Casariego et al., 2009). Film opacity was determined according to the method described by Irissin-Mangata, Bauduin, Boutevin, and Gontard (2001) on rectangular strips directly placed in a UV–vis spectrophotometer test cell. The absorption spectrum of the sample was obtained from 400 to 800 nm with a UV-Visible spectrophotometer Shimadzu 1601 PC (Tokyo, Japan). Film opacity was defined as the area under the curve divided by the film thickness and expressed as absorbance unit × nanometer/millimeter (AU nm/mm).

Color results were expressed as the average of six samples while opacity measurements were taken in triplicate for each sample.

2.2.3. Total soluble matter (TSM)

It was expressed as the percentage of the film dry mass dissolved after 24 h immersion in distilled water at room temperature (23 ± 2 °C). TSM determination was carried out according to the "wet" method proposed by Rhim, Gennadios, Weller, Cezeirat, and Hanna (1998), using distilled water (30 ml) and in the presence of sodium azide (0.02%) to prevent microbial growth. Three specimens of each film were weighed (m_h) (±0.0001 g) and then directly

immersed in distilled water under the conditions described above. After 24 h immersion, the samples were oven dried at 105 °C during 24 h, to determine the dried remnant insoluble mass (m_f). The initial moisture content was determined from specimens cut from the same film and dried at 105 °C during 24 h. The dry mass value (m_0) needed for the TSM calculations was then obtained from m_h by subtracting the initial moisture content. The TSM value was calculated as follows:

$$\text{TSM}(\%) = \frac{m_0 - m_f}{m_0} \times 100 \quad (3)$$

2.2.4. Water vapor permeability (WVP)

This value was determined gravimetrically using the ASTM Method E96-95 (ASTM, 1995). Four specimens were tested for each film type. Prior to the test, the film was placed in a chamber maintained at room temperature for 3 days at 66% RH, to ensure equilibrium conditions. Then, the film specimen was sealed on acrylic permeation cup (5 cm diameter) containing distilled water (100% RH). The cup was weighed at 1 h intervals over a 6 h period. A fan located inside the chamber was used to move the internal air ensuring uniform conditions at all test locations, being these conditions room temperature (23 ± 2 °C) and 66% RH.

2.2.5. Moisture sorption

The films, dried at 40 °C for three days in a vacuum oven, were placed inside an environmental chamber maintained at 75% relative humidity (RH) and 23 ± 2 °C, to obtain water sorption kinetics. Samples were taken out of the chamber at regular time intervals and weighed with a precision of ±0.0001 g. The equilibrium moisture content (EMC) of the films was calculated relating the weight of the samples when reached equilibrium (W_∞), which occurred after approximately 6 h of absorption of moisture, with its initial (dry) weigh (W_0), as follows:

$$\text{EMC} = \frac{W_\infty - W_0}{W_0} \times 100 \quad (4)$$

To ensure the reproducibility of the results, four specimens for each sample were tested.

2.2.6. Tensile properties

Tensile tests were performed at room temperature (23 ± 2 °C) using an Instron Universal Testing Machine model 8501. The specimens were cut according to the ASTM D1708-93 (ASTM, 1993). Five specimens from each film were tested from a minimum of three films per sample. Crosshead speed was set at 10 mm/min. The ultimate strength (σ_b), elongation at break (ε_b) and elastic modulus (E) were calculated as described in ASTM D638-94b (ASTM, 1994). Prior to running mechanical tests, films were conditioned for 48 h at 50 ± 5% RH at 25 °C.

2.2.7. Dynamic mechanical analysis (DMA)

DMA was performed using a rheometer (DMTA IV, Rheometric Scientific) in rectangular torsion mode at 1 Hz, in the temperature range from −90 to 70 °C, at a heating rate of 2 °C min^{-1}. The samples were subjected to a cyclic strain of 0.05%. This strain value was sufficiently small to ensure that the mechanical response of the specimen was within the linear viscoelastic range.

3. Results and discussion

Optical properties are essential to define the ability of films and coatings to be applied over a food surface, since they affect the appearance of the coated product, which is an important quality factor. In this work, it was noticed that addition of olive oil reduced the yellow tinge characteristic of the chitosan films, while CN cannot be distinguished, in most cases, with the unaided eye due to the excellent dispersion achieved during preparation. Thus, in order to quantify these observations, transparency measurements were carried on. Table 1 presents the opacity values reported for glycerol plasticized chitosan/nanocellulose and glycerol plasticized chitosan–olive oil/nanocellulose films. It is clearly seen that increasing CN amount (up to 7 wt.%) leads to a reduction in the opacity values of the films. At 12 wt.% CN, the opacity increases again because a clear aggregation of nanocrystals took place, which was corroborated by unaided eye observation. A plausible explanation for this fact is that when adding CN to chitosan/glycerol solution, the cellulose nanocrystals interact mainly with glycerol molecules because of their OH groups, leaving in that way less free glycerol in the glycerol rich phase and consequently, reducing the size of these domains, which leads to reduced opacity values. As it will be further explained in the following sections and was previously reported in literature (Pereda et al., 2011; Pereda, Amica, & Marcovich, 2012), chitosan–glycerol films present a phase separated film structure.

Table 1
Opacity values of nanocellulose-reinforced glycerol plasticized chitosan (CH) and glycerol plasticized chitosan–olive oil (CH + 10% OO) films.

% CN	Thickness (mm)	Opacity (UA × nm/mm)
CH		
0	0.087 ± 0.003	5389.67 ± 752.83
3	0.105 ± 0.053	4664.42 ± 1051.40
5	0.115 ± 0.046	4285.02 ± 1008.00
7	0.122 ± 0.020	3821.45 ± 1237.35
12	0.122 ± 0.035	5937.35 ± 2312.47
CH + 10% OO		
0	0.092 ± 0.018	7327.29 ± 559.97
1	0.108 ± 0.015	5540.37 ± 612.98
2	0.115 ± 0.006	5977.48 ± 450.75
3	0.142 ± 0.067	5896.39 ± 522.99

On the other hand, from the comparison of opacity values between chitosan films with and without olive oil, a clear increase of this value for lipid-containing films can be noticed. As it was indicated elsewhere (Pereda et al., 2012; Vargas et al., 2009; Villalobos, Chanona, Hernández, Gutiérrez, & Chiralt, 2005) oil droplets dispersed in the carbohydrate matrix affect the transparency by reducing the light transmitted through the resulting film. However, it is also clear that for chitosan films containing olive oil, the addition of a small CN amount (i.e. 1 wt.%) leads to a reduction of the opacity value, while further increase in the CN concentration produces a slight decrease of the transparency, probably because the nanocrystals dispersion was not as good as in the previous case. In fact, heterogeneities can be noticed with the naked eye in the film containing 3 wt.% cellulose, and more concentrated samples could not be prepared. The reduction of opacity by nanocellulose addition, although initially unexpected, could be explained considering the Pickering effect that was observed in other emulsions containing CN (Andresen & Stenius, 2007; Kalashnikova, Bizot, Bertoncini, Cathala, & Capron, 2013; Klemm et al., 2011). In this sense, it is known that if solid particles are added to a water–oil emulsion mixture, they will bind to the oil–water interface and prevent the oil droplets from coalescing, thus causing the emulsion to be more stable (Arditty, Schmitt, Giermanska-Kahn, & Leal-Calderon, 2004; Kalashnikova et al., 2013). The high stability of emulsions stabilized by colloidal particles is derived from the energy barrier required to remove the particles from the interface in order to facilitate droplet coalescence (Zoppe, Venditti, & Rojas, 2012). Properties such as hydrophobicity, shape, and size of the particle can have an effect on the stability of the emulsion (Kalashnikova et al., 2013). In other words, it is proposed that the decrease in opacity of chitosan–oil films with the addition of cellulose is due to the ability of these

Table 2
Color coordinates of nanocellulose-reinforced glycerol plasticized chitosan (CH) and glycerol plasticized chitosan–olive oil (CH + 10% OO) films.

% CN	Thickness (mm)	L^*	a^*	b^*	WI	ΔE
CH						
0	0.076 ± 0.008	76.95 ± 2.94	0.27 ± 1.11	42.28 ± 4.23	51.79 ± 4.44	0
3	0.091 ± 0.023	76.79 ± 3.78	0.15 ± 1.72	36.58 ± 6.55	56.63 ± 7.38	5.7
5	0.095 ± 0.017	75.77 ± 1.38	2.40 ± 2.30	47.49 ± 5.80	46.59 ± 5.85	5.6
7	0.098 ± 0.003	76.25 ± 0.69	2.85 ± 0.73	48.15 ± 1.02	46.23 ± 1.21	6.5
12	0.111 ± 0.017	69.52 ± 0.83	7.73 ± 3.66	51.74 ± 3.49	39.15 ± 4.51	14.2
CH + 10% OO						
0	0.107 ± 0.026	74.16 ± 2.46	2.41 ± 1.22	41.97 ± 3.46	50.40 ± 3.29	3.5
1	0.098 ± 0.008	71.96 ± 2.11	5.78 ± 2.84	49.13 ± 5.54	45.28 ± 6.59	10.1
2	0.100 ± 0.019	68.75 ± 3.72	6.29 ± 1.24	49.13 ± 1.42	41.60 ± 1.87	12.3
3	0.095 ± 0.020	74.46 ± 2.25	3.34 ± 2.33	45.19 ± 5.47	47.95 ± 5.97	4.9

nanoparticles to surround the tiny oil droplets, limiting (or preventing) their coalescence. Thus, in this system, not only chitosan but also nanocellulose is acting as emulsifier, reducing furthermore the size of oil drops, and leading to lower opacity values. In order to corroborate this statement, optical microscope pictures of chitosan/glycerol/olive emulsions without CN (A) or containing 1 wt.% of CN (B) were obtained and are presented in Fig. 1. As can be noticed, not only the sample prepared without nanocellulose presents larger oil drops than the complex suspension but also the drop size distribution is narrower in the second case.

Color coordinates were calculated from the spectral distribution of the films obtained on a standard white plate, as listed in Table 2. The differences in lightness (L^*) between the different samples are minor, with the slightly lowest values corresponding to films prepared with the addition of olive oil or a relatively high concentration of cellulose nanofibers (i.e. 12 wt.%), in which case the fibers could not be adequately dispersed. Concerning red–green (a^*), yellow–blue (b^*) and total color differences (ΔE) parameters, they clearly increase as cellulose concentration increases no matter the presence of olive oil, but being higher for films containing the lipidic phase. The films prepared with 3 wt.% nanofiber and olive oil did not follow exactly this trend, but this behavior can be attributed to the poor CNs dispersion, as previously indicated. On the other hand, whiteness (WI) values follow a decreasing tendency. Taking into account that the chromaticity components of the color space CIELab were obtained on a standard white plate, a decrease of WI and L^* values with respect to the control film may reflect a decrease of transparency or a gain of color of the films. In this sense, the incorporation of nanocellulose or olive oil contributes to strengthen the color of the films.

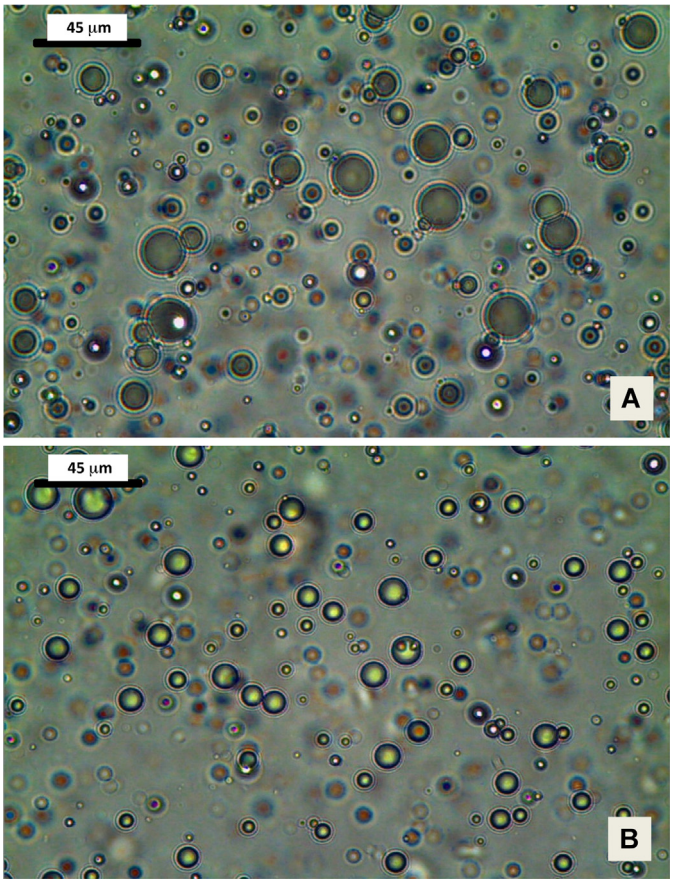

Fig. 1. optical microscope photographs of chitosan/glycerol/olive oil emulsions without CN (A) or containing 1 wt.% of CN (B).

Table 3 presents the total soluble matter in water (TSM), water vapor permeation (WVP) and contact angle values for the different films. The results showed that the water solubility decreased as both nanocellulose and olive oil concentration increased. In fact, it can be noticed that there is a synergistic effect between both additives since the TSM of the sample containing 3 wt.% CN and 10 wt.% oil is only 40% of the value corresponding to the same composite but prepared without lipid addition. These results clearly show that there is a moderate interaction among cellulose particles and chitosan, and a stronger interaction between olive oil and chitosan, as reported in other papers (Pereda et al., 2012; Vargas et al., 2009). In fact, the presence of oil not only leads to strong association with chitosan but also entraps part of the plasticizer, avoiding its loss in aqueous medium, as reported in a previous publication (Pereda et al., 2012). Due to the high degree of deacetilation of the chitosan used in this work (98%), electrostatic interaction predominates between amino group of the glucosamine units (NH_3^+) and the acid group (O–) of free fatty acids (mainly oleic acid), forming an insoluble salt, as reported elsewhere (Dimzon, Ebert, & Knepper, 2013; Wydro, Krajewska, & Hac-Wydro, 2007). Therefore, fatty acid chains anchor to chitosan by electrostatic forces, and at the same

Table 3
WVP, TSM and contact angle (θ) of nanocellulose-reinforced glycerol plasticized chitosan (CH) and glycerol plasticized chitosan–olive oil (CH + 10% OO) films.

% CN	WVP (kg m/Pa s m^2) × 10^{13}	TSM (%)	θ (°)
CH			
0	13.5 ± 6.6	14.25 ± 3.88	60.16 ± 2.35
3	10.9 ± 0.5	13.58 ± 2.91	59.20 ± 6.14
5	10.1 ± 1.4	10.81 ± 0.60	52.34 ± 3.76
7	9.0 ± 1.2	10.95 ± 0.30	53.80 ± 0.82
12	8.3 ± 1.1	7.21 ± 2.06	44.38 ± 1.11
CH + 10% OO			
0	9.4 ± 1.5	11.34 ± 0.25	64.10 ± 5.23
1	8.0 ± 0.5	7.66 ± 1.08	55.95 ± 2.06
2	8.1 ± 0.4	7.59 ± 1.33	48.98 ± 2.97
3	6.0 ± 0.2	5.46 ± 2.41	59.20 ± 4.12

time also interact via hydrophobic forces with the rest of olive oil. Moreover, the presence of CN in the emulsion films enhances this behavior, indicating a synergistic effect between both additives, which is attributed to hydrogen bonding (because of OH groups) and electrostatic interactions developed between the amino group of the glucosamine units and the sulfate ester groups ($O–SO_3^-$) anchored to the surface of the nanocrystals, as a result of the sulfuric acid hydrolysis procedure used for the preparation (Aranguren, Marcovich, Salgueiro, & Somoza, 2013; Dong, Revol, & Gray, 1998; Kalashnikova, Bizot, Cathala, & Capron, 2012).

Moreover, it is noticed that the incorporation of CN to chitosan films is enough to decrease the water vapor permeability of the composite films, due to the increasing path length for vapor diffusion. In addition, it is well known that molecules penetrate with difficulty in the crystalline domains of cellulose microfibrils. Similar results were reported by Khan et al. (2012), who indicated that water vapor permeability (WVP) of chitosan/CN films was decreased by 27% for the optimum 5 wt.% CN content. According to Casariego et al. (2009) the WVP of clay reinforced composite films was between 9 and 32% lower than that of neat chitosan. Rhim, Hong, Park, and Perry (2006) also reported that WVP of composite films decreased significantly ($p < 0.05$) by 25–30% depending on the nanoparticle used; these values being comparable with the ones obtained in the present work. Water vapor more favorably diffuses through the amorphous phase of the composite film, so the degree of crystallinity, mainly governed by the cellulose crystal concentration, is also of importance in the permeability behavior of the nanocomposite (Khan et al., 2012; Rhim et al., 2006). Furthermore, by combining both the lipidic component and the reinforcing filler, a more important reduction of this property can be achieved, as previously noticed for the water solubility value, due to the non-polar character of the oil component. The results show that the presence of oil reduced the WVP value by 30%, compared to the value obtained for the plasticized chitosan film (without CN), although a 45% reduction was noticed when comparing the effect of oil in samples containing 3% CN. In this case, the synergistic effect of both additives is again noticed. As previously indicated, the addition of oil promotes the formation of highly stable emulsions with tiny droplets stabilized by the colloidal particles, evenly distributed within the film matrix, which provides hydrophobicity and thus reduces the adsorption of water molecules, as observed in related works on emulsified films (Fabra, Pérez-Masiá, Talens, & Chiralt, 2011; Shellhammer & Krochta, 1997; Valenzuela et al., 2013).

The contact angle is one of the basic wetting properties of packaging materials, indicating the hydrophilic/hydrophobic character of the surface of the film. In our case, measurements were performed using ethylene-glycol as polar solvent. Accordingly, an increase in the contact angle indicates a density reduction of polar groups on the film surface. This trend can be noticed by comparing the values registered for the unfilled films (0 wt.% cellulose) prepared without (60.16°) and with the addition of olive oil (64.10°), as expected. However, it is clear that cellulose addition causes an increase in the superficial hydrophilicity of the reinforced samples compared to that of chitosan or chitosan–olive oil films. Regarding this point it is necessary to remember that although concentrated sulfuric hydrolysis favors defibrillation as well as removal of the amorphous or less ordered regions embedded within cellulose microfibrils, leading to highly crystalline particles (less polar than the initial cellulose source), the hydrolysis also results in substantially charged surfaces that enhance their hydrophilicity (Azizi Samir, Alloin, & Dufresne, 2005; Dong et al., 1998; Elazzouzi-Hafraoui et al., 2008). The deviation from the trend of the sample containing 3 wt.% cellulose and olive oil is attributed again to its heterogeneity.

The results for equilibrium moisture content (EMC) for the different composite films conditioned at 75% RH are shown in Fig. 2.

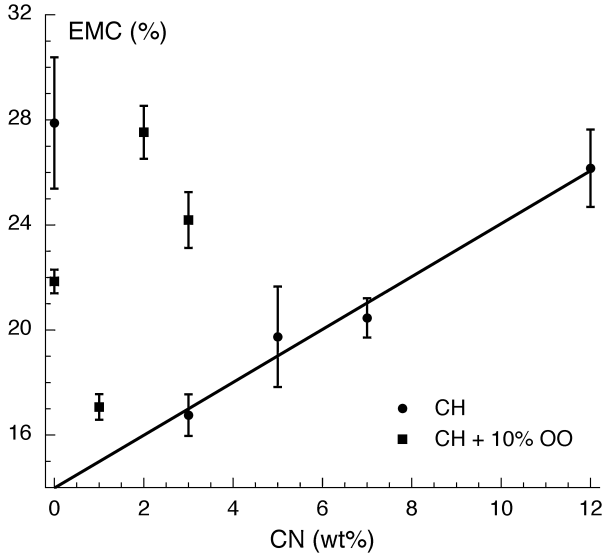

Fig. 2. Equilibrium moisture content as a function of CN concentration of nanocellulose-reinforced glycerol plasticized chitosan (CH) and glycerol plasticized chitosan–olive oil (CH + 10% OO) films.

Regarding the films prepared without olive oil, it is noticed that the addition of only 3 wt.% CN leads to a sharp drop of the moisture uptake, which is in agreement with what was expected. It is worth noting that CN was prepared by removing part of the amorphous regions, leaving the less accessible crystalline region as fine crystals, which are not involved in binding water molecules (since they are mostly impermeable). On the other hand, cellulose partially "blocks" hydrophilic sites of glycerol and chitosan (preferentially those of glycerol) by hydrogen bonds with OH groups, leaving less OH groups to interact with water molecules, resulting in lower EMC values. In this sense, the 3 wt.% CN plasticized chitosan film behaves as it was prepared with less glycerol, and consequently its hydrophilicity decreases. However, by adding higher CN contents, a linear increase of EMC was observed, which was attributed to filler aggregation, leaving in consequence relatively less suface area per crystal volume to interact with glycerol–chitosan. Similar results were found in the literature: a higher resistance of thermoplastic starch to water was reported when increasing the cellulose nanoparticle content (Anglès & Dufresne, 2000; Lu, Weng, & Cao, 2005; Svagan, Hedenqvist, & Berglund, 2009), which was ascribed to the presence of strong hydrogen bonding interactions between particles and between the starch matrix and CN. These authors also suggested that hydrogen bonding interactions in the composites tend to stabilize the starch matrix when they were submitted to highly moist atmosphere and also that the high crystallinity of cellulose could be responsible for the decreased water uptake at equilibrium. On the other hand, Garcia de Rodriguez, Thielemans, and Dufresne (2006) indicated that sisal CN addition stabilized the moisture sorption of PVAc-based nanocomposites with no benefit seen when increasing the CN content beyond the percolation threshold, i.e. the water uptake stayed constant. Moreover, they also indicated that below CN percolation threshold, stabilization was only noticed at low relative humidity, whereas high humidity results in disruption of CN–PVAc interactions. More recently, de Mesquita, Donnici, Teixeira, and Pereira (2012) indicated that their bio-based nanocomposites obtained through covalent linkage between chitosan and cellulose nanocrystals (CH–c-CNC) showed a remarkable decrease in hydrophylicity with respect to the neat chitosan, being this effect more pronounced than that obtained for the control system chitosan-unmodified nanocellulose.

Table 4
Tensile properties of of nanocellulose-reinforced glycerol plasticized chitosan (CH) and glycerol plasticized chitosan–olive oil (CH + 10% OO) films.

% CN	Modulus (MPa)	Tensile strength (MPa)	Elongation at break (%)
CH			
0	134.6 ± 16.6	8.4 ± 0.6	19.6 ± 3.4
3	237.6 ± 98.3	12.6 ± 1.1	9.2 ± 2.7
5	328.3 ± 89.1	10.7 ± 1.5	7.9 ± 3.3
7	346.7 ± 89.3	12.6 ± 1.5	7.9 ± 0.8
12	351.7 ± 164.6	8.9 ± 1.6	5.1 ± 0.9
CH + 10% OO			
0	189.3 ± 49.0	8.9 ± 2.3	13.8 ± 6.3
1	220.7 ± 43.1	8.9 ± 1.8	9.8 ± 3.5
2	360.6 ± 29.2	8.7 ± 1.8	5.9 ± 2.8
3	239.7 ± 84.1	10.5 ± 2.2	11.2 ± 2.1

The EMC of olive oil–chitosan film (without NC) was significantly lower than that of the corresponding neat plasticized chitosan matrix. It is also noted that this decrease is higher than it would be predicted from a rule of mixtures (i.e. $27.9 \times 0.9 = 25.1$ considering that oil does not absorb moisture). The diminished availability of amino groups of chitosan due to the electrostatic neutralization with the carboxylate groups of olive oil, added to the compactness of the film network may cause limited access of water molecules to hydrophilic chitosan sites, thus resulting in a decrease of equilibrium moisture content in the emulsion films, as reported in related works (Pereda et al., 2012; Vargas et al., 2009). However, when introducing nanocellulose, it turns into a very complex system and the results have a large dispersion, being the tendency not clear and still under study. Several facts should be considered to explain this behavior: the Pickering effect of CN could limit interactions between plasticized chitosan and olive oil, leading to more hygroscopic films. At the same time, cellulose has more affinity for glycerol OH groups, blocking them and leading to more hydrophobic films. Also, the aggregation of cellulose nanoparticles trying to avoid the non-polar part of the system would make it less effective in trapping hydrophilic sites; hence the resulting EMC would depend on the predominant effect in each formulation.

Fillers with excellent mechanical properties and high aspect ratio are particularly interesting because their high specific surface area enhances the filler–matrix interactions and thus, leads to a high reinforcing effect. Tensile properties reported in Table 4 reveal that CN performs as reinforcing filler for both plasticized chitosan films with and without olive oil. Indeed, the tensile modulus increased and elongation at break decreased (due to the rigid nature of the filler) as CN concentration increased.

Filler-reinforced films usually tend to become more brittle as the concentration of the reinforcing particles increases (Cyras, Manfredi, Ton-That, & Vázquez, 2008; Rhim, 2011). This behavior is also common for nanocomposite films (Khan et al., 2012). The increased tensile modulus of the CN-reinforced chitosan films is attributed to the increased stiffness of the films by the addition of CN. It is also noticed that the tensile modulus is higher for the unreinforced chitosan–olive oil film, compared to unfilled chitosan one, due to the interactions developed between lipid and carbohydrate phases, as reported in a previous publication (Pereda et al., 2012). On the other hand, it is also clear that the Young modulus increases more or less linearly for lower filler concentrations (up to 7 wt.% for chitosan films or 2 wt.% for chitosan–olive oil films), changing the trend for higher cellulose contents. This effect is attributed again to fiber agglomeration that reduces the reinforcing effect.

Regarding the tensile strength of plasticized chitosan films, it increased about 27–50% upon cellulose addition, for concentrations lower than 12 wt.%. This increase can be attributed to two factors, as reported in related papers (Khan et al., 2012): (1) the favorable nanocrystal–polymer interactions and (2) the reinforcing effect occurring through effective stress transfer at the nanocrystal–polymer interface. The interaction between the anionic sulfate groups of CN and the cationic amine groups of chitosan might favor a good interface between the matrix and the filler. This may lead to high tensile strength values for the nanocomposite films (De Mesquita, Donnici, & Pereira, 2010; Khan et al., 2012). In a similar way, de Mesquita et al. (2012) found a nearly linear increase in the tensile strength and modulus with increasing modified cellulose nanowhiskers concentration: for the nanocomposite with the highest amount of nanocrystals (60%), an increase in the tensile strength of about 150% relative to the neat chitosan was observed, while the modulus increased up to 160%. On the other hand, in our case it is clear that reaching a CN concentration of 12 wt.% cellulose nanocrystals does not help to further improve the tensile strength. The reason for this behavior can be attributed again to the aggregation of CN particles above a certain concentration, which results in no further improvement of mechanical properties. In this line, Li, Zhou, and Zhang (2009) reported excellent reinforcing properties of CN showing a 41% increase in the chitosan films's tensile strength due to the incorporation of 15–20% (w/w) nanocrystals. Jalal Uddin, Araki, and Yasuo Gotoh (2011) reported the fabrication of polyvinyl alcohol nanocomposites reinforced with different CN concentrations (up to 30%, w/w) and found the optimum nanocrystal concentration in terms of mechanical strength around 5 wt.%, while Khan et al. (2012) reported that the highest tensile strength for chitosan based films was obtained at an optimum CN loading ranging between 3 and 5 wt.%, with the strength reaching a plateau for higher CN concentrations. On the other hand, tensile strength values for chitosan/olive oil films remain practically constant with cellulose concentration, except for samples containing 3 wt.% CN. The same oil–cellulose–chitosan interactions that revealed beneficial and synergistic effects for others properties seem to neutralize in this case.

Thermo-mechanical properties of the films were also investigated and results are shown in Fig. 3(a and b). Tan δ versus temperature plot shows two relaxation processes: the relaxation processes occurring at low (between −30 and −25 °C) and high temperatures (35 °C), were associated to the glycerol- and chitosan-rich phases, respectively.

For chitosan/glycerol films the general trend is the increase of the glass transition temperature of the glycerol-rich phase (Tg_{GRP}) as the CN content increases (Fig. 3a). Cellulose crystals form, preferentially, hydrogen bonds with the OH groups of glycerol, reducing its mobility because of these physical interactions.

Also the temperature of the glycerol-poor or chitosan-rich phase (Tg_{GPP}) increases with CN addition due to the reduction on glycerol content, i.e. it consists of less plasticized chitosan, which restricts its ability to relax.

Analyzing the curves for the system with olive oil (Fig. 3b), cellulose would be associated primarily with glycerol molecules, and also it may help to the dispersion and stability of the incorporated oil (because of the Pickering effect). Increasing cellulose content reduces the temperature interval between the relaxation of the two phases, i.e. Tg_{GRP} increases and Tg_{GPP} decreases with CN addition (probably because cellulose nanofibers are compromised in oil–CN (Pickering effect) or glycerol–CN interactions and do not hinder chitosan movements, although at 3 wt.% concentration there is visible fiber aggregation and Tg increases in both phases.

On the other hand, the addition of cellulose up to 7 wt.% as the unique additive leads to an increase in the storage modulus (Fig. 3a) compared to the corresponding unfilled film, although no important further variations were noticed with increasing nanocellulose concentration. This behavior is clear in the low temperature range (i.e. −70 to 10 °C). However, at higher temperatures, the softening of the plasticized chitosan matrix masked the cellulose reinforcing

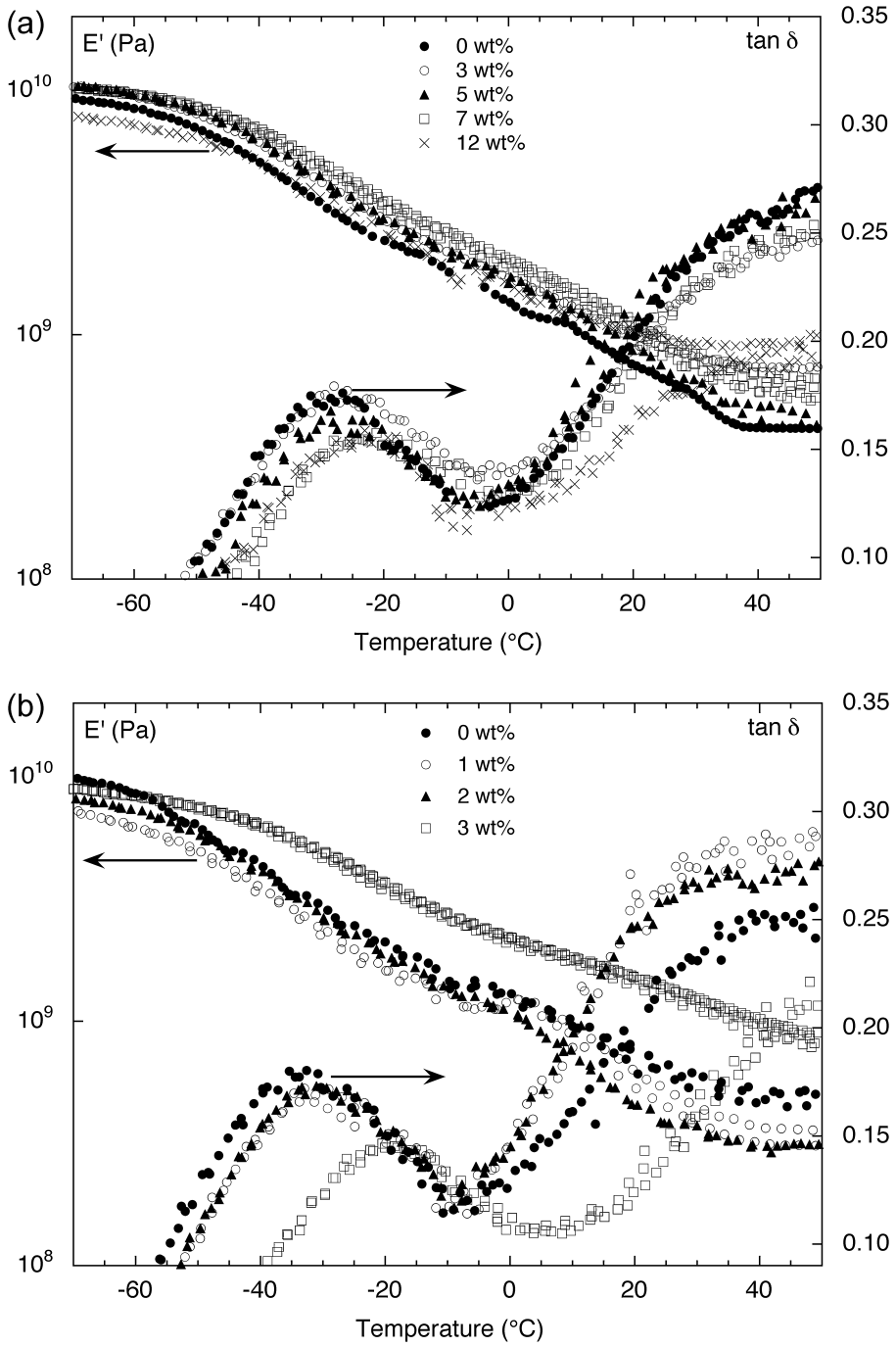

Fig. 3. Storage modulus and Tan δ versus temperature curves of a) nanocellulose-reinforced glycerol plasticized chitosan (CH) and b) glycerol plasticized chitosan–olive oil (CH + 10% OO) films.

effect and all curves tend to merge. Regarding the more complex chitosan/olive oil/cellulose system, it is noticed that the storage modulus of the films (Fig. 3b) containing 1 and 2 wt.%. cellulose were lower than that of the corresponding unreinforced system. Only the film that presents evident fiber aggregation (3 wt.%) shows the expected reinforcing effect. However, in this case, the storage modulus dependence with cellulose concentration is clear (i.e. E' increases as filler concentration increases from 1 to 3 wt.%). Probably this effect could be explained taking into account that the "effective" concentration of reinforcing cellulose was reduced due to the amount of cellulose involved in oil–CN interactions, and thus, at very low content it would act more likely as a defect rather than as reinforcement. It should be kept in mind that in this case, a dynamic deformation added to a temperature sweep was applied to the film and thus, the obtained results do not, necessarily, be comparable to tensile ones.

4. Conclusions

Complex chitosan-plasticized films modified with olive oil (OO) and/or cotton nanocrystals (CNs) were successfully obtained by casting. Although their physical, mechanical and barrier properties were strongly related with the CNs concentration and the presence (or absence) of olive oil, the films developed in this work can be used as food packaging, but also, due to the edible,

non-toxic and nutritional characteristics of the different constituents, they can also be considered as edible food packaging. Due to cellulose–glycerol–chitosan interactions, composite films appeared less opaque as the cellulose concentration increases (up to 7 wt.% CN), which is an advantage from the consumer viewpoint. Moreover, both, nanocellulose and olive oil addition leads to the reduction of the water vapor permeation and the total soluble matter, which are also desirable characteristics for a food packaging. The EMC of the chitosan plasticized matrix was considerably reduced by adding only 3 wt.% CN or only olive oil (without reinforcing filler), and thus these films could be considered for special applications.

The tensile modulus was significantly increased by CN addition, while the utilization of olive oil moderates the reduction of the elongation at break; this synergistic effect is an improvement over the expected response (i.e. modifications that lead to an increase in the stiffness, usually also lead to a decrease in the deformation capability).

Acknowledgements

The authors gratefully acknowledge the financial support provided by the National Research Council of Argentina (CONICET), grant PIP 0648, the Science and Technology National Promotion Agency (ANPCyT), grant PICT-2010-1791, the Science, Technology and Productive Innovation Ministry (MINCyT), grant ECOS-SUD and the National University of Mar del Plata (Project # 15/G312).

References

Andresen, M., & Stenius, P. (2007). Water-in-oil emulsions stabilized by hydrophobized microfibrillated cellulose. *Journal of Dispersion Science and Technology*, *28*, 837–844.

Anglès, M. N., & Dufresne, A. (2000). Plasticized starch/tunicin whiskers nanocomposites. 1. Structural analysis. *Macromolecules*, *33*, 8344–8353.

Aranguren, M. I., Marcovich, N. E., Salgueiro, W., & Somoza, A. (2013). Effect of the nano-cellulose content on the properties of reinforced polyurethanes. A study using mechanical tests and positron annihilation spectroscopy. *Polymer Testing*, *32*, 115–122.

Arditty, S., Schmitt, V., Giermanska-Kahn, J., & Leal-Calderon, F. (2004). Materials based on solid stabilized emulsions. *Journal of Colloid and Interface Science*, *275*(2), 659–664.

ASTM. (1993). *Standard test method for tensile properties of plastics by use of microtensile specimens, standards designation: D1708 Annual book of ASTM standards*. Philadelphia, USA: ASTM.

ASTM. (1994). *Standard test method for tensile properties of plastics, standards designation: D638 Annual book of ASTM standards*. Philadelphia, USA: ASTM.

ASTM. (1995). *Standard test methods for water vapor transmission of materials. Standards designation: E96-95 Annual book of ASTM standards*. Philadelphia, USA: ASTM.

Azizi Samir, M., Alloin, F., & Dufresne, A. (2005). Review of recent research into cellulosic whiskers, their properties and their application in nanocomposite field. *Biomacromolecules*, *6*(2), 612–626.

Cagri, A., Ustunol, Z., & Ryser, E. T. (2004). Antimicrobial edible films and coatings. *Journal of Food Protection*, *67*(4), 833–848.

Cao, X., Chen, Y., Chang, P. R., Muir, A. D., & Falk, G. (2008). Starch-based nanocomposites reinforced with flax cellulose nanocrystals. *Polymer Letters*, *2*(7), 502–510.

Casariego, A., Souza, B. W. S., Cerqueira, M. A., Teixeira, J. A., Cruz, L., Díaz, R., et al. (2009). Chitosan/clay films' properties as affected by biopolymer and clay micro/nanoparticles' concentrations. *Food Hydrocolloids*, *23*, 1895–1902.

Cyras, V. P., Manfredi, L. B., Ton-That, M.-T., & Vázquez, A. (2008). Physical and mechanical properties of thermoplastic starch/montmorillonite nanocomposite films. *Carbohydrate Polymers*, *73*(1), 55–63.

De Mesquita, J. P., Donnici, C. L., & Pereira, F. V. (2010). Biobased nanocomposites from layer-by-layer assembly of cellulose nanowhiskers with chitosan. *Biomacromolecules*, *11*(2), 473–480.

de Mesquita, J. P., Donnici, C. L., Teixeira, I. F., & Pereira, F. V. (2012). Bio-based nanocomposites obtained through covalent linkage between chitosan and cellulose nanocrystals. *Carbohydrate Polymers*, *90*, 210–217.

Dieter-Klemm, D., Schumann, D., Kramer, F., Hessler, N., Koth, D., & Sultanova, B. (2009). Nanocellulose materials: Different cellulose, different functionality. *Macromolecular Symposia*, *280*, 60–71.

Dimzon, I. K. D., Ebert, J., & Knepper, T. P. (2013). The interaction of chitosan and olive oil: Effects of degree of deacetylation and degree of polymerization. *Carbohydrate Polymers*, *92*, 564–570.

Dong, X. M., Revol, J. F., & Gray, D. G. (1998). Effect of microcrystallite preparation conditions on the formation of colloid crystals of cellulose. *Cellulose*, *5*(1), 19–32.

Elazzouzi-Hafraoui, S., Nishiyama, Y., Putaux, J. L., Heux, L., Dubreuil, F., & Rochas, C. (2008). The shape and size distribution of crystalline nanoparticles prepared by acid hydrolysis of native cellulose. *Biomacromolecules*, *9*(1), 57–65.

Fabra, M., Pérez-Masiá, R., Talens, P., & Chiralt, A. (2011). Influence of the homogenization conditions and lipid self-association on properties of sodium caseinate based films containing oleic and stearic acids. *Food Hydrocolloids*, *25*, 1112–1121.

Favier, V., Chanzy, H., & Cavaille, J. Y. (1995). Polymer nanocomposites reinforced by cellulose whiskers. *Macromolecules*, *28*, 6365–6367.

Fernandes, S. C. M., Freire, C. S. R., Silvestre, A. J. D., Pascoal Neto, C., Gandini, A., Berglund, L. A., et al. (2010). Transparent chitosan films reinforced with a high content of nanofibrillated cellulose. *Carbohydrate Polymers*, *81*, 394–401.

García, M. A., Pinottia, A., Martino, M. N., & Zaritzky, N. E. (2004). Characterization of composite hydrocolloid films. *Carbohydrate Polymers*, *56*(3), 339–345.

Garcia de Rodriguez, N. L., Thielemans, W., & Dufresne, A. (2006). Sisal cellulose whiskers reinforced polyvinyl acetate nanocomposites. *Cellulose*, *13*, 261–270.

Gennadios, A., Weller, C. L., Hanna, M. A., & Froning, G. W. (1996). Mechanical and barrier properties of egg albumen films. *Journal of Food Science*, *61*(3), 585–589.

Ghanbarzadeh, B., & Almasi, H. (2011). Physical properties of edible emulsified films based on carboxymethyl cellulose and oleic acid. *International Journal of Biological Macromolecules*, *48*, 44–49.

Irissin-Mangata, J., Bauduin, G., Boutevin, B., & Gontard, N. (2001). New plasticizers for wheat gluten films. *European Polymer Journal*, *37*, 1533–1541.

Jalal Uddin, A., Araki, J., & Yasuo Gotoh, Y. (2011). Toward strong green nanocomposites: Polyvinyl alcohol reinforced with extremely oriented cellulose whiskers. *Biomacromolecules*, *12*, 617–624.

Kalashnikova, I., Bizot, H., Cathala, B., & Capron, I. (2012). Modulation of cellulose nanocrystals amphiphilic properties to stabilize oil/water interface. *Biomacromolecules*, *13*, 267–275.

Kalashnikova, I., Bizot, H., Bertoncini, P., Cathala, B., & Capron, I. (2013). Cellulosic nanorods of various aspect ratios for oil in water Pickering emulsions. *Soft Matter*, *9*, 952–959.

Khan, A., Khan, R. A., Salmieri, S., Le Tien, C., Riedl, B., Bouchard, J., et al. (2012). Mechanical and barrier properties of nanocrystalline cellulose reinforced chitosan based nanocomposite films. *Carbohydrate Polymers*, *90*, 1601–1608.

Klemm, D., Kramer, F., Moritz, S., Lindstrom, T., Ankerfors, M., Gray, D., et al. (2011). Nanocelluloses: A new family of nature-based materials. *Angewandte Chemie International Edition*, *50*(24), 5438–5466.

Kowalczyk, D., & Baraniak, B. (2011). Effects of plasticizers, pH and heating of film forming solution on the properties of pea protein isolate films. *Journal of Food Engineering*, *105*, 295–305.

Kunte, L. A., Gennadios, A., Cuppett, S. L., Hanna, M. A., & Weller, C. L. (1997). Cast films from soy protein isolates and fractions. *Cereal Chemistry*, *74*(2), 115–118.

Li, Q., Zhou, J., & Zhang, L. (2009). Structure and properties of the nanocomposite films of chitosan reinforced with cellulose whiskers. *Journal of Polymer Science Part B: Polymer Physics*, *47*(11), 1069–1077.

Lu, Y., Weng, L., & Cao, X. (2005). Biocomposites of plasticized starch reinforced with cellulose crystallites from cottonseed linter. *Macromolecular Bioscience*, *5*, 1101–1107.

Monedero, F. M., Fabra, M. J., Talens, P., & Chiralt, A. (2009). Effect of oleic acid–beeswax mixtures on mechanical, optical and water barrier properties of soy protein isolate based films. *Journal of Food Engineering*, *91*, 509–515.

Muzzarelli, R. A. A., Tarsi, R., Filippini, O., Giovanetti, E., Biagini, G., & Varaldo, P. E. (1990). Antimicrobial properties of N-carboxybutyl chitosan. *Antimicrobial Agents and Chemotherapy*, *34*, 2019–2023.

Muzzarelli, R. A. A. (2010). Chitins and chitosans as immunoadjuvants and non-allergenic drug carriers. *Marine Drugs*, *8*(2), 292–312.

Muzzarelli, R. A. A., Boudrant, J., Meyer, D., Manno, N., DeMarchis, M., & Paoletti, M. G. (2012). A tribute to Henri Braconnot, precursor of the carbohydrate polymers science, on the chitin bicentennial. *Carbohydrate Polymers*, *87*, 995–1012.

Ojagh, S. M., Rezaei, M., Razavi, S. H., & Hosseini, S. M. H. (2010). Development and evaluation of a novel biodegradable film made from chitosan and cinnamon essential oil with low affinity toward water. *Food Chemistry*, *122*(1), 161–166.

Pereda, M., Amica, G., & Marcovich, N. E. (2012). Development and characterization of edible chitosan/olive oil emulsion films. *Carbohydrate Polymers*, *87*, 1318–1325.

Pereda, M., Ponce, A. G., Marcovich, N. E., Ruseckaite, R. A., & Martucci, J. F. (2011). Chitosan–gelatin composites and bi-layer films with potential antimicrobial activity. *Food Hydrocolloids*, *25*, 1372–1381.

Perez-Gago, M., Rojas, C., & Del Rio, M. (2002). Effect of lipid type and amount of edible hydroxypropyl methylcellulose–lipid composite coatings used to protect postharvest quality of mandarins cv. fortune. *Journal of Food Science*, *67*(8), 2903–2910.

Rhim, J., Gennadios, A., Weller, C. L., Cezeirat, C., & Hanna, M. A. (1998). Soy protein isolate-dialdehyde starch films. *Industrial Crops Products*, *8*, 195–203.

Rhim, J., Hong, S., Park, H., & Perry, K. W. (2006). Preparation and characterization of chitosan-based nanocomposite films with antimicrobial activity. *Journal of Agricultural and Food Chemistry*, *54*, 5814–5822.

Rhim, J.-W. (2011). Effect of clay contents on mechanical and water vapor barrier properties of agar-based nanocomposite films. *Carbohydrate Polymers*, *86*(2), 691–699.

Shellhammer, T., & Krochta, J. (1997). Whey protein emulsion film performance as affected by lipid type and amount. *Journal of Food Science*, *62*(2), 390–394.

Svagan, A. J., Hedenqvist, M. S., & Berglund, L. (2009). Reduced water vapour sorption in cellulose nanocomposites with starch matrix. *Composites Science and Technology*, *69*, 500–506.

Tanada-Palmu, P., & Grosso, C. (2005). Effect of edible wheat gluten-based films and coatings on refrigerated strawberry (*Fragaria x ananassa*) quality. *Postharvest Biology and Technology*, *36*, 199–208.

Valenzuela, C., Abugoch, L., & Tapia, C. (2013). Quinoa protein–chitosan–sunflower oil edible film: Mechanical, barrier and structural properties. *LWT – Food Science and Technology*, *50*, 531–537.

Vargas, M., Albors, A., Chiralt, A., & González-Martínez, Ch. (2009). Characterization of chitosan–oleic acid composite films. *Food Hydrocolloids*, *23*, 536–547.

Villalobos, R., Chanona, J., Hernández, P., Gutiérrez, G., & Chiralt, A. (2005). Gloss and transparency of hydroxypropil methylcellulose films containing surfactants as affected by their microstructure. *Food Hydrocolloids*, *19*, 53–61.

Wydro, P., Krajewska, B., & Hac-Wydro, K. (2007). Chitosan as a lipid binder: A Langmuir monolayer study of chitosan–lipid interactions. *Biomacromolecules*, *8*(8), 2611–2617.

Zoppe, J. O., Venditti, R. A., & Rojas, O. J. (2012). Pickering emulsions stabilized by cellulose nanocrystals grafted with thermo-responsive polymer brushes. *Journal of Colloid and Interface Science*, *369*(1), 202–209.